

## Effect of Solid Phase and Geometry on Liquid Velocity of Three-Phase Bubble Columns

Karina K. Costa\*, Diana I. Sanchez-Forero, Rodrigo L. Amaral, Osvaldir P. Taranto, Milton Mori

School of Chemical Engineering at University of Campinas (UNICAMP), Albert Einstein ave., 500 – Zip Code: 13083-852, Campinas, SP, Brazil.  
[karinakc@feq.unicamp.br](mailto:karinakc@feq.unicamp.br)

Multiphase flows have a large applicability in the industry and its studies are very important. One example of three-phase system is bubble columns operating with solid phase as catalyst in the process. In this context the hydrocracking systems are used to process heavy oil and are becoming very common at oil refineries. Its operation is done in multiple-stage each one in a different reactor. In this work, it is proposed a new geometry of bubble columns in which two different solid phases are considered inside the system. The technique used in this work is Particle Image Velocimetry (PIV) in which it is possible to measure velocity fields inside the columns without interfering with the flow. Rhodamine B is a tracer for the liquid phase and the PIV is extended to the Fluorescent Stereo-PIV using two CCDs cameras that allow estimating the third component velocity. In this work it is analyzed the fluid dynamic of the liquid phase inside a three-phase bubble column with expansion of diameter when compared with a traditional bubble column with cylindrical geometry. The liquid phase is water at 22 °C, FCC catalyst with diameter of 100-125  $\mu\text{m}$  and air as gas phase injected at the bottom with constant flow set at 1.5 L/min. Besides, the two column geometries present different positions and the experimental results show the input of different solid concentration inside the system to analyze the influence over the liquid phase average velocity field. The comparison of two columns with different solid concentration is presented and discussed.

### 1. Introduction

The hydrocracking process at oil industry is used to convert heavy distillation residue in lighter compounds. This is very attractive to the because of the minimization of unconverted residual oil and purification of the product that result in low sulfur and deeply purified. The three-phase (gas-liquid-solid) hydrocracking can operate in multiple-stage configuration where two or more reactors are used. In these units the first stage does an initial cracking and removes the contaminants using a high activity catalyst and the unconverted oil goes to a different reactor (Sommerfeld, Bröder, 2009).

One visualization technique very used to analyze flows is Particle Image Velocimetry (PIV). This allows viewing and quantifying instantaneous velocity field without interfering with the flow. The system relates pairs of images taken with a high resolution camera synchronized with a laser light in a way that the object plane in study coincides with the illuminated range of the flow. This technique can be extended using two cameras that record the fluid from different directions and allow reconstructing the third component velocity (Raffel et al, 1998). This variation is named Stereo-PIV and it was used in this work.

In order to reduce the number of reactor in this process, this work uses a modified geometry with two diameters connected that allows to have two different solid phases inside the reactor. In this work it was performed an initial analysis of the fluid dynamic inside the column with one solid phase compared with the two-phase system. The gas flow and solid load are very low so the PIV images obtained had great quality.

## 2. Experimental Setup

In the present work it was used two column geometries built of transparent acrylic that allows optical access inside the flow. The first one consists in a cylinder with 14.5 cm of diameter and it is referred as Column 1. The second has two tubes with diameters of 14.5 cm and 24.5 cm and it is referred as Column 2. Both columns have 100 cm of height and were filled initially with 80 cm of liquid phase, water at 22 °C. Figure 1 presents an overview of the experimental system, where: (a) is the Column 2 with diameter expansion, laser system, box with known aperture, CCD cameras positions (vertical line fixed); (b) is the system top view of Stereo-PIV arrangement for experiments 1b-6b; (c) the gas plate distributor with 21 holes; (d) is the Column 1 cylindrical and CCD cameras positions (horizontal line fixed); and (e) is the system top view of Stereo-PIV arrangement for experiments 1a-6a.

Although it is possible to use two different solid phases inside the Column 2, the experiments presented here were done using only gas-liquid and adding FCC catalyst with a diameter range of 100-125  $\mu\text{m}$  in both columns. The gas phase is air at 22 °C entering the column through a plate distributor with 21 holes distributed in a central square array. Glass spheres with 2 mm of diameter were positioned immediately before the plate to ensure a better distribution of the gas inside the column. Involving the cylinder it was placed a square acrylic box filled with water at 22 °C to reduce the distortions occurred by the cylindrical curvature of the system wall capable of producing images with better quality.

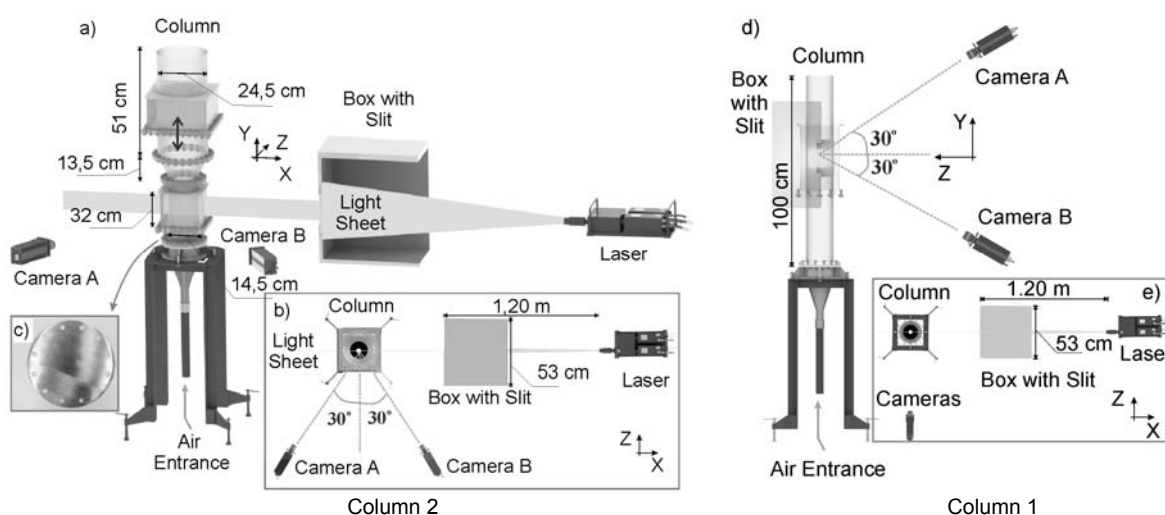


Figure 1: Experimental system overview

The Stereo-PIV system used was developed by Lavis and consisted in a laser Nd:YAG with 200 mJ/pulse  $\lambda = 532 \text{ nm}$ , and two Charge Couple Device (CCD) cameras synchronized by an internal unit PTU-9. The recording frequency was 4.92 Hz. Each camera has an objective lens with focal length of 60 mm model Nikon Micro-Nikor ( $f\#2.8D$ ) and it was coupled a high-pass filter to allow only the passage of a wavelength close to the tracer. The cameras were placed in an angular configuration at the same horizontal position when used the Column 1 and same vertical position with the Column 2. The first configuration allows the same illumination intensity of the flow for both cameras but it was not possible to use it in the Column 2 because of its geometry. To control the light thickness it was used a box with a slit of 4 mm located 1.20 m from the laser system. The calibration procedure was done to reduce the wall distortions problems and the calibration average error was 0.85 pixel. The tracer particle used was Rhodamine B with diameter of 20-50  $\mu\text{m}$ ,  $\lambda = 620 \text{ nm}$ ,  $\rho = 1100 \text{ kg/m}^3$  and maximum Stokes number of  $2 \times 10^{-5}$ . According Brandon and Aggarwal (2001), particles with  $St < 0.1$  can be used as tracers because its behavior is similar of a fluid.

The images obtained were preprocessed using a filter RMS (Roots Mean Square)  $3 \times 3$  pixels and then the cross-correlation procedure was applied in which there was an interrogation strategy with two steps, one of 256 pixels (25 % overlap of adjacent windows) and the second of 128 (50 % overlap). The quality of Stereo-PIV measurement was ensured by the cross-correlation coefficient and peak ratio that were upper 0.5 and 2. In the post processing was used the median test to remove the spurious vectors in velocity field with a removal threshold of 2 and a neighborhood of  $3 \times 3$  pixels (Westerweel and Scarano, 2005).

The gas phase was set at 1.5 L/min and the range time between the frame 0 and 1 used was 5.000-8.000  $\mu\text{s}$  adjusted according each height of measure and solid load able to obtain a tracer particle displacement around

5-15 pixels. The distance of the measure window center and the plate distributor of gas phase and the amount of FCC catalyst added at the system are presented at Figure 2 and Table 1.

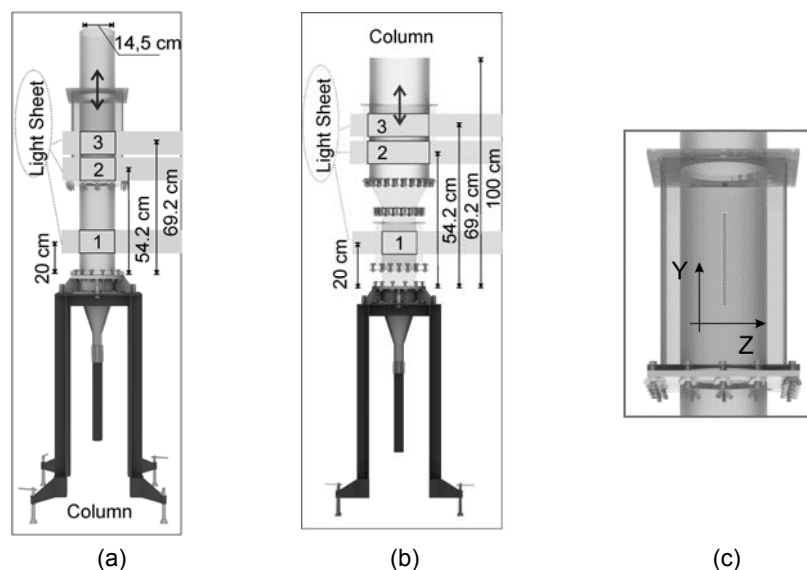


Figure 2 – Measurement y-axis positions for (a) Column 1 – experiments 1a-6a; (b) Column 2 – experiments 1b-6b; (c) measurement z-axis position

Table 1: Distance of the measure window center and the plate distributor of gas phase and the amount of FCC catalyst added at the system

Cylindrical bubble column (Column 1)			Bubble column with diameter expansion (Column 2)		
Experiment	Amount of solid (g)	Measurement position (mm)	Experiment	Amount of solid (g)	Measurement position (mm)
1a	0	200	1b	0	200 (inferior diameter)
2a	0	542	2b	0	570 (superior diameter)
3a	0	692	3b	0	692 (superior diameter)
4a	10g	200	4b	10g	200 (inferior diameter)
5a	10g	542	5b	10g	542 (superior diameter)
6a	10g	692	6b	10g	692 (superior diameter)

The images were taken in three different vertical positions in compared to the gas distributor (Table 1) and the measuring windows were approximately 14.5 x 10 cm. The mean resolution of the system was 9 and 12 pixels/mm for Columns 1 and 2, respectively. At the superior part of the Column 2, two horizontal parallel measurement windows were obtained and the results superimposed to include the full diameter of the column. The time of experiment for all cases was 4.000 images that correspond to about 17 min to minimize the errors and ensure that the flow was stable.

### 3. Results

The results for all the experiments present the y component of the liquid phase velocity inside the systems. The velocity  $V_y$  fields for Column 1 are presented in the Figures 3 – 5. Recirculation zones can be perceived in the velocity fields. The Figure 3 illustrates the top of the Column 1 were there are two recirculation areas close to the system walls and it is possible to see that the solid load increases the maximum region of liquid velocity at the center (Figure 3b). This can occur because the solid tend to stay close to the regions were the velocity is lower because the wall effects causing a bigger resistance in these regions allowing the bubbles to pass through the center with higher velocity.

When the three heights analyzed are compared, it is possible to observe that the velocity increases according to the bottom distance (Figures 3-5). This occurs because the bubbles at the bottom have more liquid resistance to ascend and higher pressure. As it ascends in the column the quantity of liquid above is smaller so the gas phase rises with more velocity and, by consequence, the liquid velocity is greater.

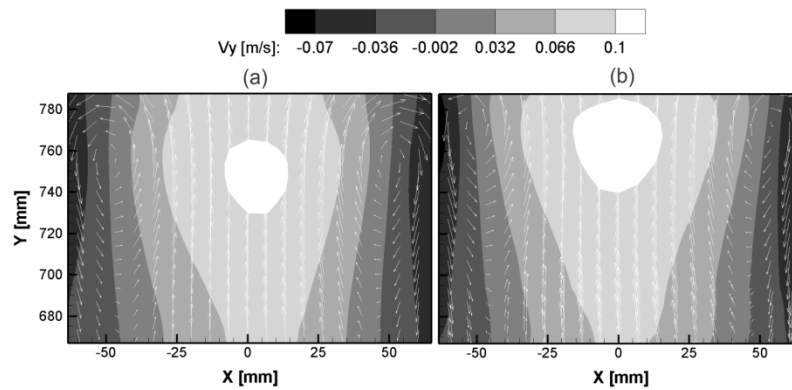


Figure 3: Velocity fields of  $V_y$  component for experiments 3a and 6a: (a) Column 1 two-phase (h3) and (b) Column 1 three-phase (h3)

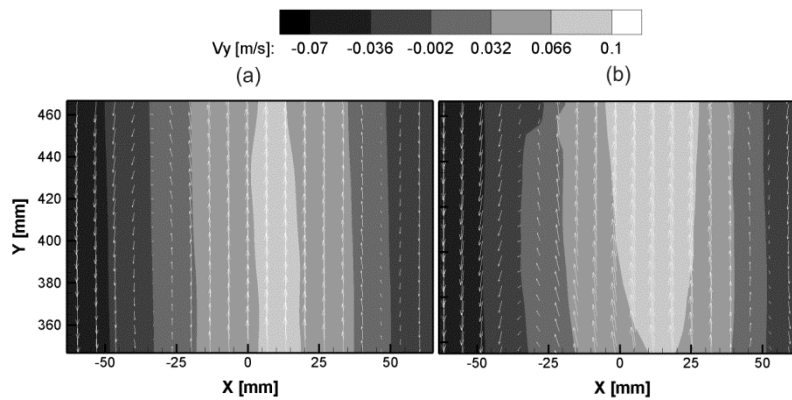


Figure 4: Velocity fields of  $V_y$  component for experiments 2a and 5a: (a) column 1 two-phase (h2) and (b) column 1 three-phase (h2)

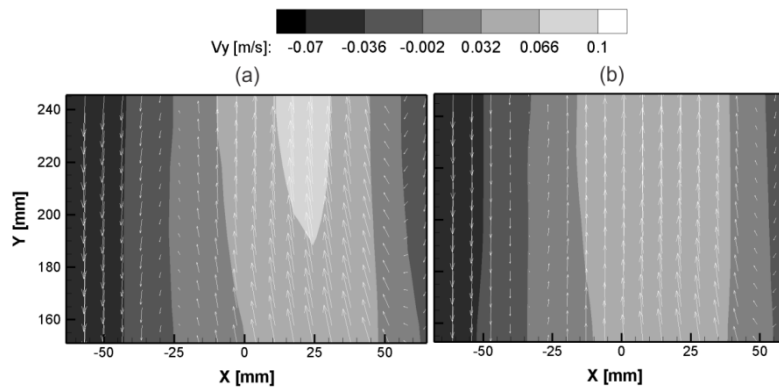


Figure 5: Velocity fields of  $V_y$  component for experiments 1a and 4a: (a) column 1 two-phase (h1) and (b) column 1 three-phase (h1)

The Column 2 results were obtained in both, superior (Figures 6 and 7) and inferior diameters (Figure 8). The results show that the y component of velocity increases as the bubbles ascend in the system. This is explained as in the Column 1, at the bottom the quantity of fluid above is bigger as well as the fluid resistance so when the gas phase goes upward the resistance reduces and the velocity is higher. The maximum velocity of liquid phase at the bottom of the column is about 0.04 m/s in both two and three-phase cases, whereas at

the top position it reaches 0.1 m/s for two-phase and 0.08 m/s for three-phase systems presenting an increase up to 60 %.

The velocity fields for two and three-phases height of 150 – 250 mm (Figure 8) shows that the higher velocities are at the right side of the column 2. This occurs because the low distance and flow rate of the gas input. As the distance from the gas plate distributor increases, the profile tends to dislocate toward the column center. But because the column has a diameter expansion it is possible to see a large recirculation at the left side of the two-phase case (Figure 6a). The bubbles can take a preferred path following the inferior diameter and ascend at the right side causing the recirculation in about half of the diameter. The solid load reduces this effect. It is possible to observe in Figure 6b that the region of higher velocity is close to the center of the column. The solid phase diluted in the superior diameter offers a resistance more distributed in this region and the gas phase ascends at the center where there is lower influence of the wall.

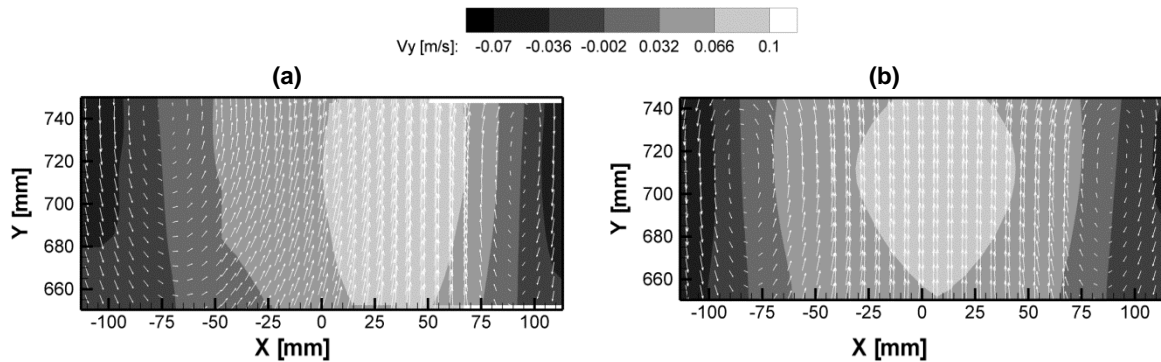


Figure 6: Velocity fields of  $V_y$  component for experiments 3b and 6b: (a) column 2 two-phase (h3) and (b) column 2 three-phase (h3)

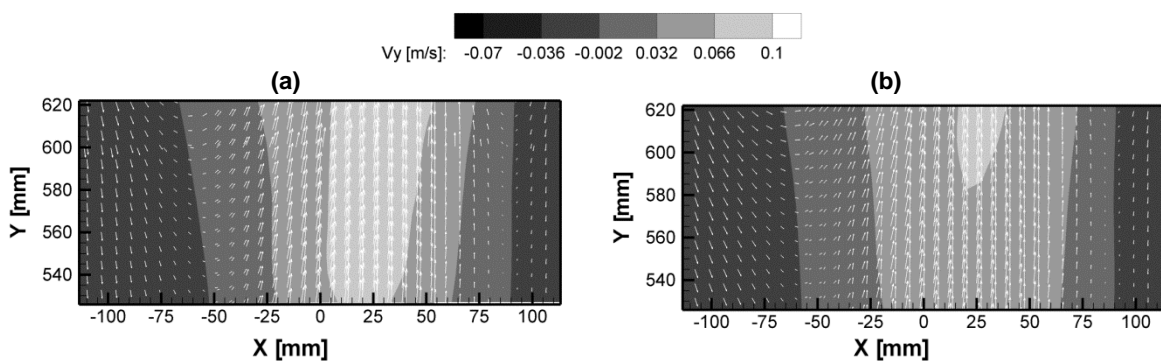


Figure 7: Velocity fields of  $V_y$  component for experiments 2b and 5b: (a) column 2 two-phase (h2) and (b) column 2 three-phase (h2)

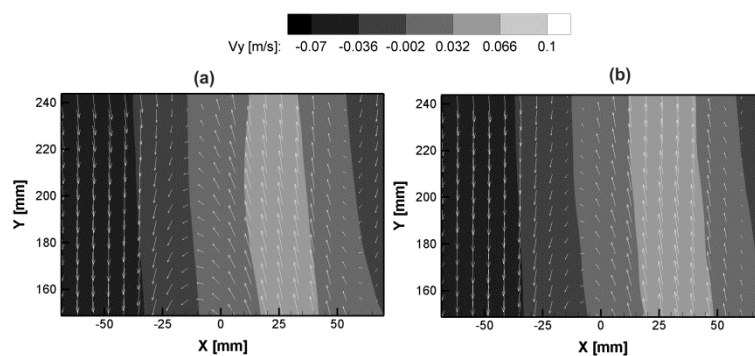


Figure 8: Velocity fields of  $V_y$  component for experiments 1b and 4b: (a) column 2 two-phase (h1) and (b) column 2 three-phase (h1)

The results of Column 1 for the height of 600 and 740 mm (Figure 9) show a typical bubble column profile with upward velocity at the center and downward velocity close to the column walls for two and three-phase cases (M. Sommerfeld, and D. Bröder, 2009). But it is not symmetrical in the cases closer to the gas plate distributor (Figure 9a,b). This can be explained by the very low gas input (1.5 L/min). The bubbles take a preferred path at the right side where the liquid velocity presents higher values. The adding of solid phase at the Column 1 results in a change of the velocity profile where the flow is not developed reducing the values and dislocating slightly the profile toward the column center (Figure 9a). The solid effect is not perceived at the top of the Column 1 where the flow is developed (Figure 9c).

Because of the diameter expansion, the quantity of liquid added to the system is greater in Column 2 than Column 1 and as consequence, the velocity profiles (Figure 9) show that the upward velocities of liquid phase are higher in the Column 1 for the heights studied.

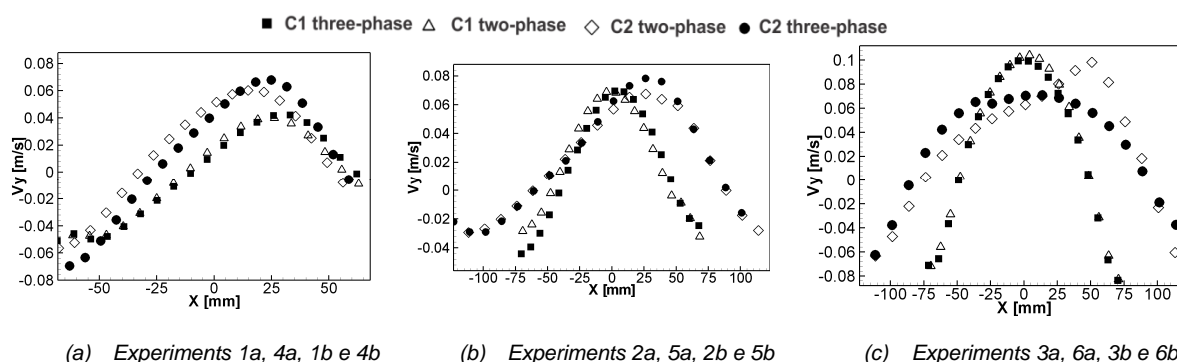


Figure 9: Velocity profiles of  $V_y$  component for experiments with Columns 1 and 2, two and three-phase: (a) height of 200 mm from the gas plate distributor; (b) 600 mm; (c) 740 mm

#### 4. Conclusions

The experiments show that the solid phase and geometry studied caused changes in the ascendant liquid phase velocity. In all cases the velocity profiles presented higher values toward the columns centers and descendant velocities near the walls. Although the solid load and gas input are very low, it is possible to observe that the Column 2 geometry presents lower velocities and the solids dispersed in the flow cause resistance for the upward displacement of the bubbles.

#### Acknowledgements

The authors are grateful to Petroleo Brasileiro S.A. (PETROBRAS) for the financial support that makes this work possible.

#### References

- Morel F., Kressmann S., Harle V., Kasztelan S., 1997, Processes and Catalysts for Hydrocracking of Heavy Oil and Residues. Studies in Surface Science and Catalysis, 106, 1–16.
- Raffel M., Willert C., Kompenhans J., 1998, Particle image velocimetry: a practical guide. Springer, Berlin, Germany.
- Robinson P.R., Dolbear G.E., 2006, Hydrotreating and Hydrocracking: Fundamentals. Springer Science And Business Media, Inc., 7, 177-218.
- Sommerfeld M., Bröder D., 2009, Analysis of Hydrodynamics and Microstructure in a Bubble Column by Planar Shadow Image Velocimetry. Ind. Eng. Chem. Res., 48 (1), 330-340.
- Westerweel J., Scarano F., 2005, Universal outlier detection for PIV data. Experiments in Fluids, 39, 1096-1100.